Computers & Graphics 35 (2011) 92–98

Contents lists available at ScienceDirect

Computers & Graphics

journal homepage: www.elsevier.com/locate/cag

Technical Section

Facial hexahedral mesh transferring by volumetric mapping based on harmonic fields

Meng-fei Li, Sheng-hui Liao*, Ruo-feng Tong*

State Key Laboratory of CAD and CG, Department of Computer Science and Engineering, Zhejiang University, Hangzhou, China

ARTICLE INFO

Article history:
Received 24 June 2010
Received in revised form
26 October 2010
Accepted 18 November 2010
Available online 23 November 2010

Keywords:
Facial soft tissue
Hexahedral mesh
Harmonic field

ABSTRACT

Hexahedral mesh has obvious mechanical advantages over tetrahedral mesh, but it is no trivial task to generate hexahedral mesh for complex object shapes such as individual faces. This paper presents a novel method to generate patient-specific hexahedral meshes of facial soft tissue models, based on a volumetric cross-parameterization mapping from a standard hexahedral mesh to the individual model. The volumetric parameterization is constructed based on triple of the volumetric harmonic fields, which are adapted to be as close to mutually orthogonal as possible, to achieve some quasi-conformal effect. In addition, some piecewise constraints on the harmonic fields are added to ensure anatomical feature correspondence. Experimental results show that our approach works efficiently for facial soft tissue modeling, avoids element flipping and preserves mesh element angles to a significant extent.

© 2010 Elsevier Ltd. All rights reserved.

1. Introduction

The use of the finite element method for biomechanical analysis has increased rapidly in recent years. For human bodies and organs, the main obstruction to such applications is the difficulty in constructing reliable finite element models. Owing to the complex shapes of biomechanical models, significant time and effort are required to construct reasonable finite element meshes.

There are two main classes of elements used for 3D solid finite element modeling, tetrahedral and hexahedral elements, each with their own advantages and disadvantages. Tetrahedral elements are geometrically versatile and can be reliably generated by many automatic meshing algorithms [1–3], even for models of complex shapes. On the other hand, a hexahedral mesh of good quality can vastly reduce the number of elements and, consequently, reduce the analysis and post-processing times. Compared with tetrahedra, hexahedra have better convergence and sensitivity to mesh orientation. In addition, hexahedral elements are more suited for non-linear analysis and for situations when the alignment of elements is important to the physics of the problem, such as in computational fluid dynamics or simulation of anisotropic materials.

So far, a number of hexahedral meshing approaches have been proposed: feature-based [4], medial surface subdivision [5] [6], plastering [7], grid-based [8], whisker weaving [9], etc. These traditional methods are mainly designed for regular CAD models and are not well suited for biomechanical models with irregular and complex shapes.

Furthermore, it is hard for direct meshing methods to generate appropriate mesh structures for biomechanical models with important anatomical features, e.g., the eyes, nose and mouth on the facial model. The underlying constraints that make hexahedral meshing difficult are presented by Shepherd and Johnson [10]. A promising solution to address the problem is to build some generic or standard mesh model of high quality one time, with all the manual effort necessary, and then conform and adapt it to patient-specific biomechanical models. The mesh-matching method [11], which is based on the elastic registration technique, is used to adapt the generic facial hexahedral mesh model to a patient-specific morphology [12]. However, this approach can produce flipped and self-intersected elements, requiring post-treatment algorithms and even manual modifications to detect and correct mesh element irregularity.

Another kind of mapping-based meshing method is to use a parameterization technique [13–17]. Gu et al. presented a robust method to compute harmonic volumetric maps based on a meshless boundary method [18], which depends on the initial boundary surface mapping and produces a good tetrahedral mesh. He et al. [19] proposed Green's function to parameterize star shaped volume domains inspired by the electric field of point charges to generate hexahedral mesh. However, He et al.'s method is not suitable for soft facial tissues, which do not resemble a star shape. Kraevoy and Sheffer [20] introduced a shape preserving cross-parameterization method for the compatible remeshing of 3D models. Recently, Martin et al. [21] proposed a volumetric parameterization method to fit a single trivariate B-spline. Lévy and Liu [22] introduced Lp-Centroidal Voronoi Tessellation for hexahedral dominant

* Corresponding authors. Postal address: Department of Computer Science and Engineering, Zhejiang University, Hangzhou, Zip Code 310027, China.
Tel.: +86 0571 87951247.
E-mail addresses: shliao@zju.edu.cn, lshenghui@gmail.com (S.-h. Liao), trf@zju.edu.cn (R.-f. Tong).

0097-8493/$ - see front matter © 2010 Elsevier Ltd. All rights reserved.
doi:10.1016/j.cag.2010.11.013

volume meshing. These automatic meshing methods do not utilize the standard hexahedral mesh to generate appropriate mesh structures for facial anatomical features.

Given an individual facial soft tissue represented initially by a tetrahedral mesh, the goal of this paper is to investigate a convenient method to produce a specific facial hexahedral mesh. The method generates a hexahedral mesh by mapping from a standardized facial hexahedral mesh of high quality and focuses on preserving the mesh element shape as well as important anatomical features.

In Section 2, we briefly discuss our design considerations. The details of our work are explained in Section 3. In Section 4, experimental results are reported and discussed. Finally, we present our conclusion in Section 5.

2. Design considerations

As mentioned above, it is difficult to generate hexahedral mesh structures directly for biomechanical models with irregular and complex shapes. In dealing with facial soft tissue models, it is especially hard to generate appropriate mesh structures for important anatomical features, such as the eyes, nose and mouth. Thus, the best solution is to generate the individual hexahedral mesh by working from a standardized hexahedral mesh that is based on volumetric mapping. Obviously, the volumetric mapping employed should retain the element shape qualities as much as possible; so conformal parameterization, which preserves angles, is a natural choice. For the mesh deformation domain, Huang et al. [23,24] introduced a shell generation and deformation algorithm that minimizes the difference between the deformation gradient and its orthogonal part. Given a closed two-manifold and the user-specified thickness, Han et al. proposed a method to construct a layered hexahedral mesh for shell objects via a volumetric polycube map [25]. For the surface domain, Gu and Yau [16] proposed an approach to construct conformal parameterizations for surface meshes, which takes advantage of the fact that the gradient fields of the conformal parameterization are holomorphic one-forms. The holomorphic one-forms can be represented as pairs of harmonic and orthogonal gradient vector fields and calculated automatically from the surface topology structure. However, there is no theoretical agreement about what the conformal volumetric parameterization should be for general volumetric domain.

In this paper, we present a method to construct the volumetric parameterization for special volumetric domains such as soft facial tissue regions, which construct triple of the orthogonal (or as nearly so as possible) harmonic volumetric fields, to achieve some quasi-conformal mapping effect. With the volumetric cross-parameterization mapping, we can adapt a standard hexahedral mesh to the patient-specific morphology. Fig. 1 shows a building block diagram that describes our overall system.

First, we construct a standard hexahedral mesh of high quality, which has appropriate mesh structures for all the important anatomical features, such as the eyes, nose and mouth, and can be reused later for all the patient-specific facial models.

Then, we construct volumetric parameterizations for both the standard model and the personalized facial model. The key issue here is how to construct the set of three harmonic volumetric fields, which can be used as the gradient fields of the volumetric parameterization,. that is, these harmonic fields need to be as close as possible to be mutually orthogonal. Furthermore, it is important to ensure correspondence to anatomical features, such as the eyes, nose and mouth.

Finally, using the same volumetric parameterization domain, we combine these two volumetric parameterizations, with one of them reversed, to create the volumetric mapping from the standard model to personalized facial model, which is then employed to generate the desired patient-specific hexahedral mesh.

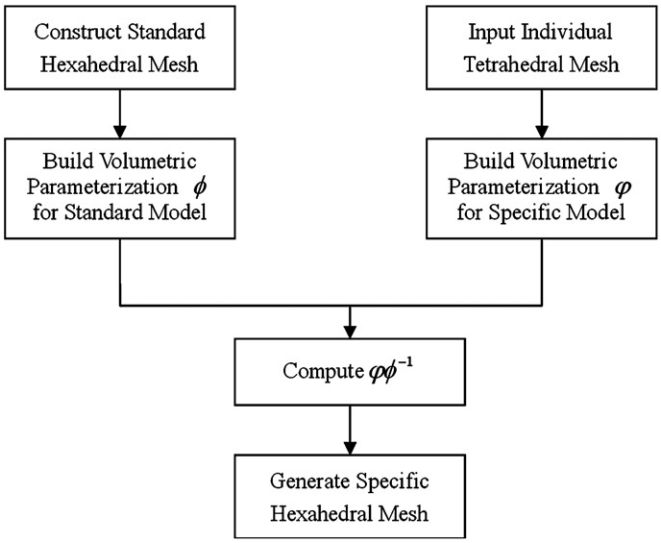

Fig. 1. Building blocks diagram for our overall system.

3. System description

3.1. Constructing a standard hexahedral mesh

The human facial soft tissue is a complicated shape, with important anatomical features, such as the eyes, nose and mouth. The automatic generation of appropriate hexahedral mesh structures for these regions is very difficult. Therefore, we designed some interactive and semi-automatic tools to create, together with manual modification methods, a standard hexahedral mesh of high quality. Note that the standard hexahedral mesh is constructed only once and will be used repeatedly for all patient-specific facial models. We believe that the need for manual interaction here will not restrict the applicability of our method.

As one usually focuses on the frontal region of the facial model when simulating physical behavior, we ignore the soft tissue above the forehead and behind the ears, as shown in Fig. 2. Loosely speaking, this makes the facial soft tissue region appear roughly like a bended thin cuboid, with three obvious axes: from left to right, from bottom to top and from inside to outside. These axes can be used as appropriate boundary conditions later to generate three quasi-conjugate harmonic fields.

Our semi-automatic modeling tool also takes advantage of this configuration, which can be further improved by quadrilateral meshing methods [26,27]. An initial quadrilateral mesh for the outer surface of the standard facial triangular model input is generated by cutting operations. Vertical and horizontal curves are produced by plane sections and connected to generate the initial quadrilateral mesh. Because there is no need for dense hexahedral meshes, a sparse quadrilateral mesh composed of 700 quadrilaterals is created. Then regions of significant anatomical features, such as the eyes, nose and mouth, are carefully modified to achieve a more appropriate mesh structure and preserve the anatomical features. Note that a few triangular elements are manually inserted to improve the adjacent quadrilateral quality and obtain a more appropriate mesh structure, but this will not lead to problems in post-processing and is common in finite element analysis.

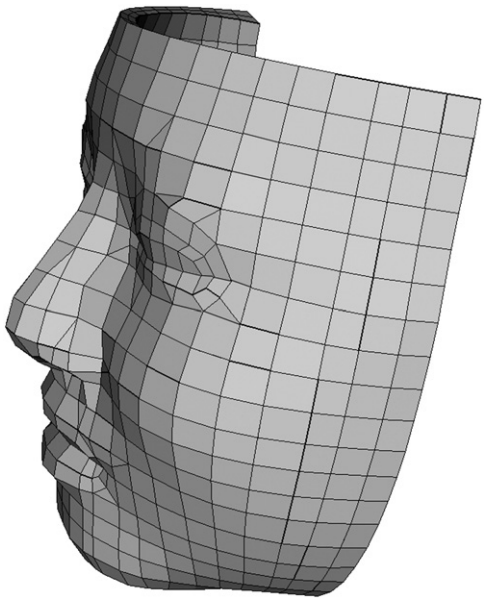

Fig. 2. Standard hexahedral mesh.

Once the outer quadrilateral mesh is created, we push the mesh into the inner surface, mainly along the surface's normal directions. A certain amount of manual work is then done to improve the resulting inner quadrilateral mesh. Finally, the intermediate layers are interpolated, and the hexahedral elements are constructed. Fig. 2 shows the resulting hexahedral dominant mesh, which contains 1248 elements and an average element quality of 0.715, according to the hexahedral shape metric introduced in [28].

3.2. Computing the volumetric harmonic field

A harmonic field is a solution to the Laplace equation

$$\Delta f(x, y, z) = 0 \tag{1}$$

subjected to some Dirichlet boundary conditions. One standard way to obtain the harmonic field is to solve the Laplace equation using the finite element method. Another more efficient method is to obtain and apply the discretization of the volumetric Laplacian operator directly.

Unlike the surface Laplacian operator, the volumetric Laplacian operator for tetrahedral mesh is described only in a few published studies [29–31]. For the typical vertex-based discretization of the Laplacian operator, $\Delta f_i = \sum_{j \in N(i)} w_{ij}(f_i - f_j)$, Meyer et al. [29] first observed that the volumetric edge weight is proportional to the cotangents of dihedral angles. Then Wang et al. [30] deduced the operator based on a harmonic energy and set the edge weight as $w_{ij} = (1/12)\sum_{k=1}^{n} l_k \cot(\theta_k)$, where $l_k = l_{pq}$ is the length of the edge (p,q) to the opposite edge (i,j) and $\theta_k = \theta_{pq}$ is the dihedral angle. Liao et al. [31] recently deduced the volumetric operator based on its basic definition, $\Delta f \equiv div(\nabla f)$, and set the edge weight as $w_{ij} = (1/6)\sum_{k=1}^{n} l_k \cot(\theta_k)$. However, these weighting schemes do not take varying vertex densities into account and may lead to unnatural results for irregular meshes.

To make the simulation as accurate as possible, we employ additional per-vertex normalization weights, $1/|\Omega_i|$, as in the surface case [29], where $|\Omega_i|$ is the volume of the Voronoi cell of vertex i. Taken together, the normalized volumetric Laplacian operator can be formulized as

$$\Delta f_i = \frac{1}{|\Omega_i|}\left(\frac{1}{6}\sum_{k=1}^{n} l_k \cot(\theta_k)\right)(f_i - f_j) \tag{2}$$

Because the volumetric Laplacian operator is defined only on a tetrahedral mesh, an auxiliary tetrahedral mesh is produced directly from the standard hexahedral mesh, preserving all hexahedral mesh vertices in order to transfer the corresponding harmonic field values later. Note that the auxiliary tetrahedral mesh has greatly varying vertex densities because it is converted from the hexahedral mesh with many anatomical features such as the eyes, nose and mouth; thus, the additional per-vertex normalization weights are necessary to create smooth and accurate harmonic fields. Concerning facial soft tissue modeling, our experiments demonstrate that an input tetrahedral mesh with average mesh edge length of 2 mm usually works well to produce a smooth harmonic field.

Suppose there are N vertices in the mesh, the global volumetric Laplacian operator can be represented as an $N \times N$ matrix L:

$$\mathbf{L}_{ij} = \begin{cases} \sum_{v_k \in N(i)} w_{ik}, & if\ i = j \\ -w_{ij}, & if\ j \in N(i) \\ 0, & \text{otherwise} \end{cases} \tag{3}$$

Thus we obtain a linear system

$$\mathbf{Lu} = 0 \tag{4}$$

where $u = u_0, u_1, \ldots, u_{n-1}$ are the unknown harmonic values at the corresponding vertices. To solve the system, one must specify some Dirichlet boundary conditions. This is of course not a problem, as we need to define certain boundary conditions to control the direction of resulting harmonic field. More specifically, we set the minimal scalar value (0) on boundary vertices at one end of the shape and set the maximal scalar value (1) on boundary vertices at the other end. Then, according to the maximum principle of harmonic fields, the harmonic scalar values will vary smoothly from the minimal end to the maximal end. Fig. 3(a) shows the harmonic field value distribution on an ellipsoid, where the blue (respectively red) colors represent high (respectively low) scalar values, and the marked points indicate boundary conditions. The gradient vector field of the harmonic field can also be calculated to represent the field directions explicitly.

Note that facial soft tissue has an irregular and complex shape, with important anatomical features such as the eyes, nose and mouth. In addition, different people have anatomical features of various shapes and sizes. Thus, generating harmonic fields for different facial models based solely on shape end boundary

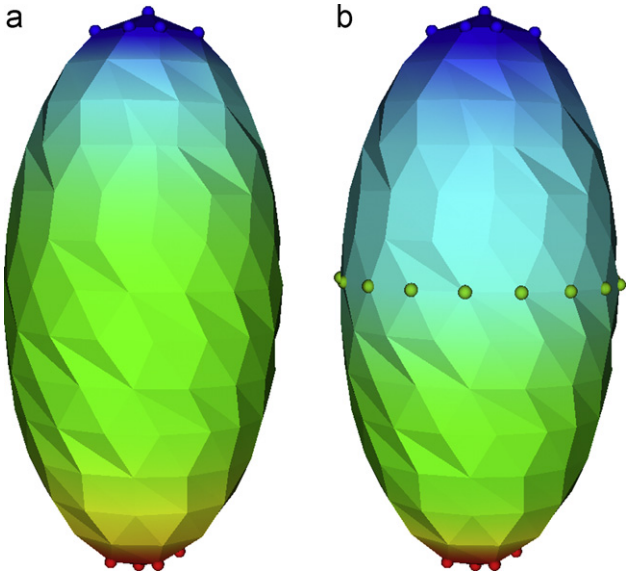

Fig. 3. Use additional piecewise constraint to control harmonic field value distribution.

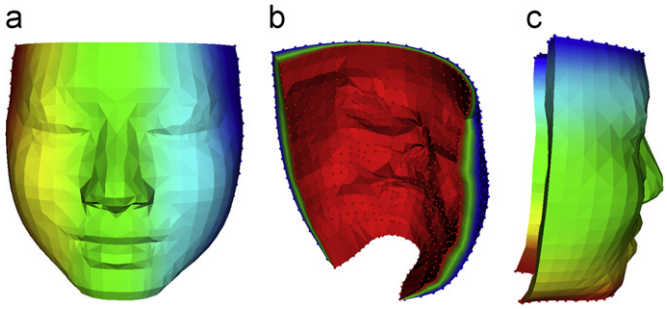

Fig. 4. Three harmonic fields on the standard model, with different directions: (a) from left to right, (b) from inner to outer and (c) from bottom to top.

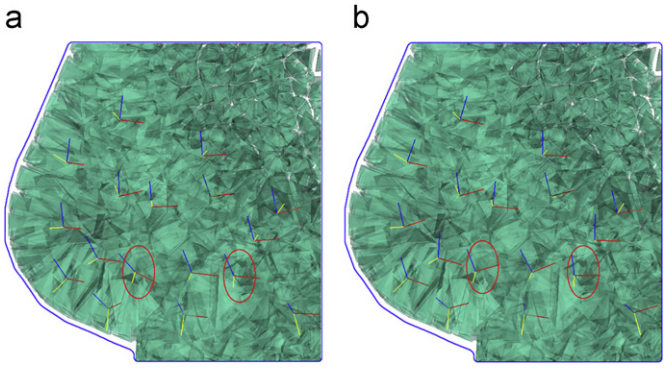

Fig. 5. Gradient vector fields before conjugation improvement (a) and after improvement (b).

conditions may produce different field values for analogous anatomical features. To ensure anatomical feature correspondence, we applied additional piecewise constraints to modify the harmonic field value distribution. Fig. 3(b) shows that the middle piecewise constraints pull the high scalar values down, where the green marked points are constrained to have the value 0.7.

3.3. Constructing the volumetric parameterization

As noted in Section 3.1, we focused only on the front region of the facial model, and made the facial soft tissue region resemble a bended thin cuboid, with its obvious three directions: from left to right, from bottom to top and from inside to outside. This provides a natural choice of setting the shape end boundary conditions. Fig. 4(a–c) show the three harmonic fields on the standard facial model, where the marked points indicate boundary conditions. Because the boundary values at the ends of the shape in each direction are set as 0 or 1, each mesh vertex now has a triple of values $(u,v,w)\in[0,1][0,1][0,1]$, and these values are most likely unique. In other words, we get a natural volumetric parameterization from the unit cube domain [0,1][0,1][0,1] to the volumetric mesh.

Note that there is no need to calculate the gradient vector fields of the harmonic scalar fields first and then integrate them to form the volumetric parameterization. The directions of the three harmonic fields, which are generated solely based on three groups of specially defined shape end boundary conditions, may not be very close to be mutually orthogonal in some complex regions, such as the nose region, as shown in Fig. 5(a), where the transparent green background represents tetrahedral elements and the three color segments indicate the direction vectors within the element. Thus, we need a scheme to improve the conjugation of the three harmonic fields to make the volumetric parameterization closer to a conformal parameterization.

A natural way to make the three fields mutually orthogonal is to first calculate their gradient vector fields, then, at each volumetric mesh element, choose one direction gradient vector as the basic vector, project the second gradient vector (preserving the vector norm) to the local plane normal to basic vector, and then take the cross product to correct the direction of the third gradient vector. Note that the three modified vector fields are now perfectly orthogonal to each other, while the corresponding potential scalar fields are no longer harmonic fields.

To address this problem, for each field, we designed a quadratic optimization to recover a new harmonic field $\mathbf{u}'$ with a gradient vector field $\nabla\mathbf{u}'$, which is as close as possible to the above modified vector field

$$\mathbf{g}^*_{\mathbf{u}} : \mathbf{u}' = \underset{u'}{\operatorname{argmin}} \sum_j V_j \left\| \nabla\mathbf{u}' - \mathbf{g}^*_{\mathbf{u}} \right\|^2 \tag{5}$$

where V_j is the volume of the tetrahedral element j. The normal equation is the discretized Poisson equation:

$$\mathrm{L}u' = \mathbf{G}^{\mathbf{T}}\mathbf{M}\mathbf{g}^*_{\mathbf{u}} \tag{6}$$

where **G** is the global volumetric gradient operator matrix and **M** is the diagonal "mass" matrix of the volumes of the tetrahedra.

Finally, the same shape end Dirichlet boundary conditions are applied to solve the Poisson equation (Eq. (6)) to recover the new harmonic fields. To construct more orthogonal fields, we apply six iterations of the orthogonal improvement process. The corresponding gradient vector fields can be calculated to demonstrate the improvement of conjugation of the three harmonic fields. Fig. 5(b) shows that the conjugation of the gradient vector fields is much better than in the previous situation; for instance, the angles between the gradient vectors are closer to perpendicular to each other, particularly in the red-circled elements. Fig. 6 shows the histogram of the angles between gradient vectors, where the red (resp. blue) pillars represent the orthogonality before (resp. after) the conjugation improvement. The histogram shows that the orthogonal improvement process brings more angles closer to right angles, which indicates the fields are more orthogonal. Overall, we constructed the volumetric parameterization in a two-stage process: first we computed three harmonic fields with shape boundary conditions as well as line constraints, and then we improved their orthogonality to bring the parameterization closer to a conformal parameterization.

3.4. Mapping the hexahedral mesh

We can now generate volumetric parameterizations for the standard facial hexahedral mesh, as well as some new individual facial meshes. Given a patient-specific facial model represented as a tetrahedral mesh, we must first manually set the shape end boundary conditions and piecewise constraints to compute three harmonic fields, and then improve the orthogonality of the fields that comprise the volumetric parameterization. Assuming that the parameterization for the standard facial mesh is $\phi : [0,1]\times[0,1]\times[0,1]\rightarrow M_S$, and that the parameterization for the patient-specific facial mesh is $\varphi : [0,1]\times[0,1]\times[0,1]\rightarrow M_P$, the volumetric mapping from the standard facial model to the patient-specific model $f : M_S \rightarrow M_P$ is given by $\varphi\phi^{-1}$.

The volumetric mapping is then employed to generate the desired patient-specific hexahedral mesh. In practical implementations, there is no need to construct a global volumetric mapping. Instead, we locally map each mesh vertex of the standard hexahedral mesh to the patient-specific model, that is, in the common unit cube domain, we implement the following procedure recurrently: find the parameterized tetrahedral element of the patient-specific model corresponding to each parameterized vertex of the standard hexahedral mesh. Mapping hexahedral vertex for the patient-specific model is then interpolated by a linear combination of the four vertex coordinates with the corresponding barycentric coordinates. The searches are completed in a breadth-first search (BFS) manner, starting from the tetrahedral element found in the previous step, proceeding to each of its

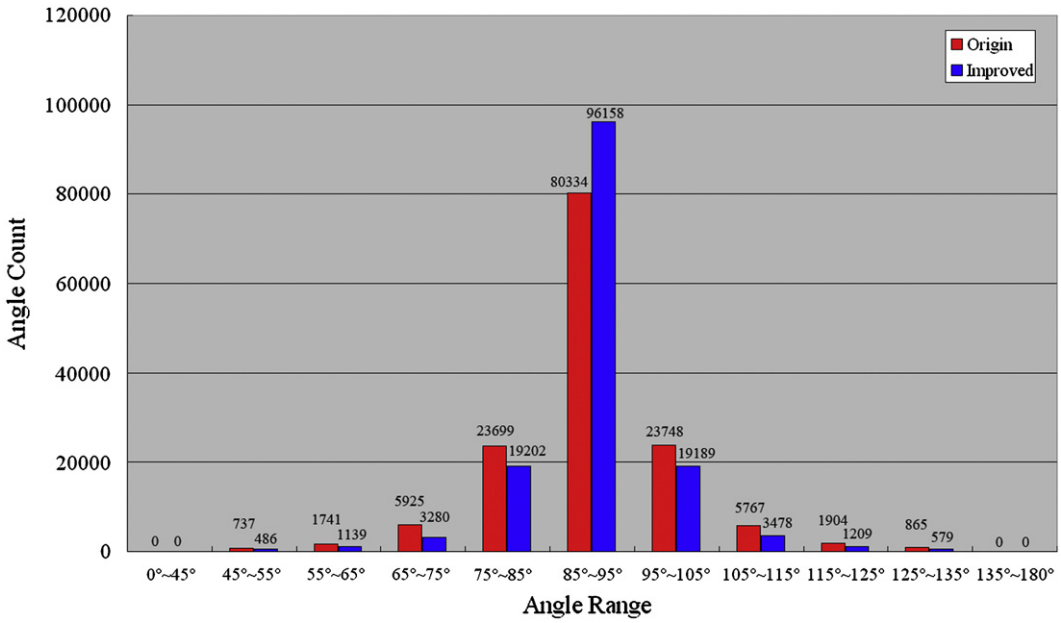

Fig. 6. Distribution of angles between gradient vectors before conjugation improvement (red) and after improvement (blue). (For interpretation of the references to colour in this figure legend, the reader is referred to the web version of this article.)

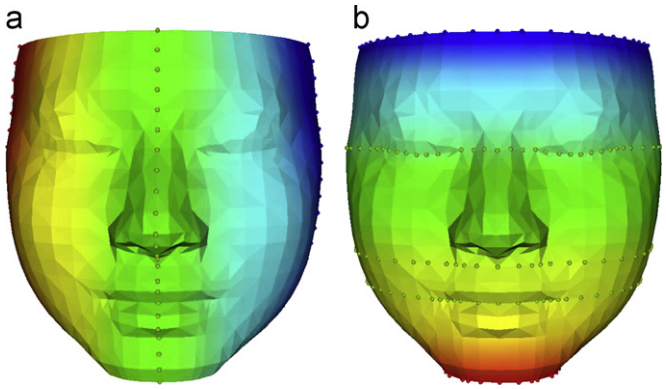

Fig. 7. Middle symmetric constraint (a) and anatomical feature constraints (b) on standard model.

neighbors. The first search is to scan the personalized tetrahedral mesh directly. Loosely speaking, we combined the mesh topology of the standard hexahedral model and the geometrical position of the personalized facial model to generate the patient-specific hexahedral dominant mesh.

As pointed out before, different people have anatomical features of various shapes and sizes. To ensure anatomical feature correspondence on the face model, some piecewise constraints were added to adjust the harmonic field value distribution. Fig. 7(a–b) shows two direction harmonic fields, where the green marked points indicate piecewise constraints on the standard facial model. The middle line constraint on the left to right direction ensures the symmetry of the facial mesh. Moreover, we also marked the eyebrow line, the middle lip line and nose-below line as piecewise constraints to ensure that these anatomical feature areas are not mismatched. These constraints are all selected by an interactive plane, which is convenient to use. Note that all the calculations for the standard facial model need to be done only once.

4. Experiments

For any new individual facial model, we set up the shape end Dirichlet boundary conditions as well as the piecewise feature constraints, as shown in Fig. 8. To ensure anatomical feature correspondence, the piecewise constraints on the specified model should be consistent with the standard model, which is shown as green marked points in Fig. 7(a–b). Then the algorithm will automatically generate triple of the harmonic and nearly orthogonal volumetric fields to form a volumetric parameterization for the patient-specific model. Together with the reversed volumetric parameterization for the standard mesh model, the composite volumetric mapping is employed to generate the patient-specific hexahedral mesh, as illustrated in Fig. 9(a–b).

The experiments were performed on an Intel Core2Quad 2.4 GHz computer with 2 GB RAM. The input individual tetrahedral mesh shown in Fig. 8 has 48,813 tetrahedrons. The volumetric parameterization procedure takes about 13,527 ms, of which the harmonic field creation process occupies about 20% and the orthogonality improvement process occupies about 80%. The facial hexahedral mesh mapping procedure takes about 11,437 ms. Thus, the total computation time is less than half a minute.

For comparison, we implemented the mesh-matching method [11] [12], which has been applied to map and generate facial hexahedral meshes. On the same input model, this method takes about 6 min, and the resulting hexahedral mesh is shown in Fig. 9(c–d).

We defined the dihedral angle distortion as the change in corresponding dihedral angles between standard and generated meshes, which illustrates how far the quality of the produced mesh deviates from the standard hexahedral mesh. Statistical analysis on the dihedral angle distortion shows that our approach preserves the mesh element shape much better than the mesh-matching method, as demonstrated in Table 1, where we can observe that about 90% of the dihedral angles are deformed by less than 16° in our method, while there are only about 53% such angles in the mesh-matching method. The average dihedral angle distortions of the two methods are 6.8° and 18.6° and the maximum angle distortions are 56° and 98°. In other words, the mesh-matching method produced flipped or self-intersected elements, as reported by Chabanas et al. [12], and the results required some post-treatment and even manual modifications to detect and correct irregular elements. However there was no need for post-treatment in our method as the flipped elements occurred very rarely.

In addition, in the mesh-matching method, the elastic transformation is evaluated by optimizing a disparity function based on the distance between the two surfaces, which results in many surface mesh vertices that deviate from the patient model. In contrast, our volumetric mapping method ensures that all surface mesh vertices are precisely on the patient model, and it, therefore, better preserves the original geometric shape of the patient-specific facial model. To make our method more convincing, we applied our approach to eight different individual facial models. The average hexahedral element qualities for each facial model are shown in Table 2, where the element qualities are measured by the hexahedral shape metric [28]; the first individual model is shown in Figs. 8–9. The statistical results indicate that the average element qualities of our method are better than those of the mesh-matching method. Fig. 10 (a–b) (resp. Fig. 11 (a–b)) shows the

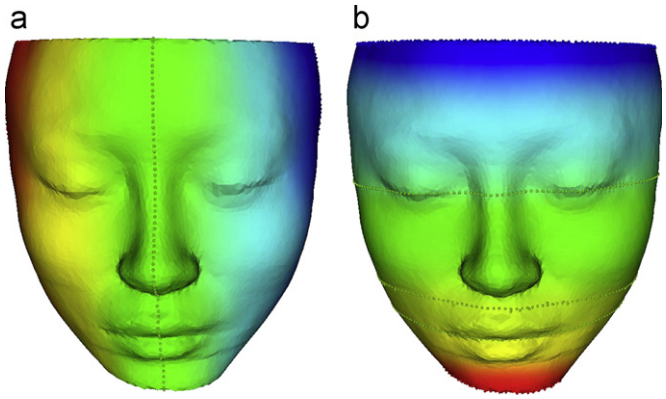

Fig. 8. Middle symmetric constraint (a) and anatomical feature constraints (b) on individual model.

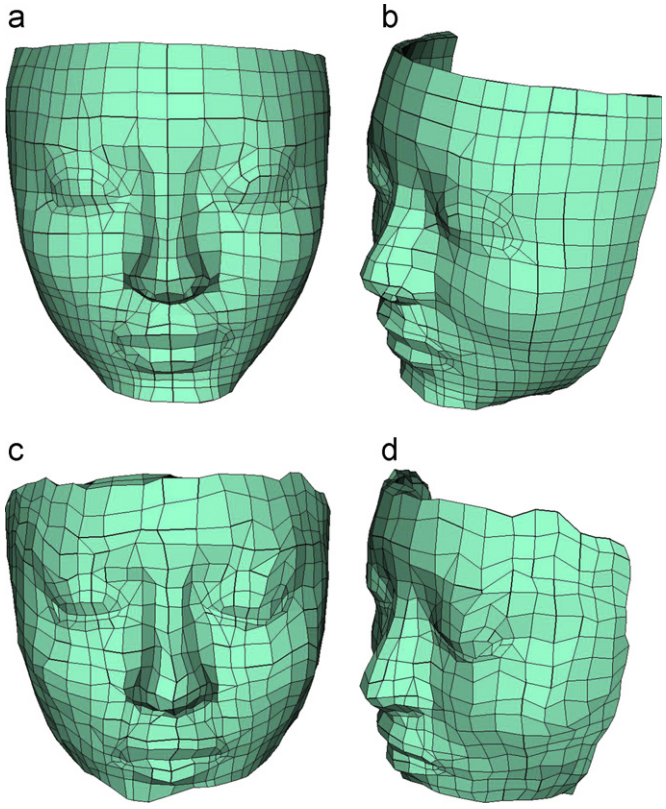

Fig. 9. Patient-specific hexahedral mesh of individual facial soft tissue using our approach (a–b) and mesh-matching method (c–d).

Table 1
Dihedral angle distortions of the mapping.

	Our method (%)	Mesh-matching method (%)
0–4°	47.0	15.7
4–16°	43.9	37.7
16–25°	5.3	18.8
25–36°	2.3	14.1
36–49°	1.0	8.3
> 49	0.5	5.4
Maximum	57	98
Average	6.8	18.6

Table 2
Experiment results on eight different facial models.

Facial models	Tetrahedral number	Average element shape quality	
		Our method	Mesh-matching method
#1	48,813	0.678	0.554
#2	37,859	0.674	0.539
#3	40,106	0.689	0.558
#4	45,698	0.672	0.547
#5	36,962	0.667	0.536
#6	40,207	0.671	0.531
#7	37,493	0.682	0.563
#8	39,658	0.676	0.548

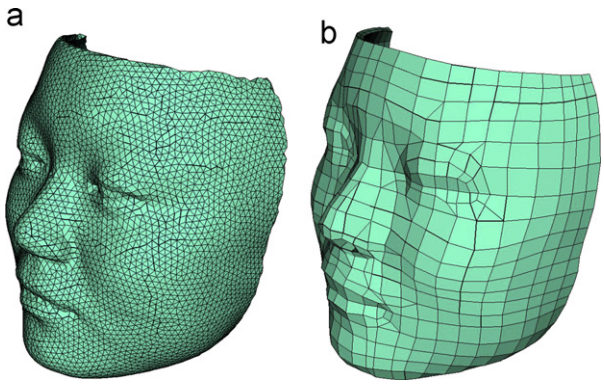

Fig. 10. Second individual facial model (a) and its hexahedral meshing result with our approach (b).

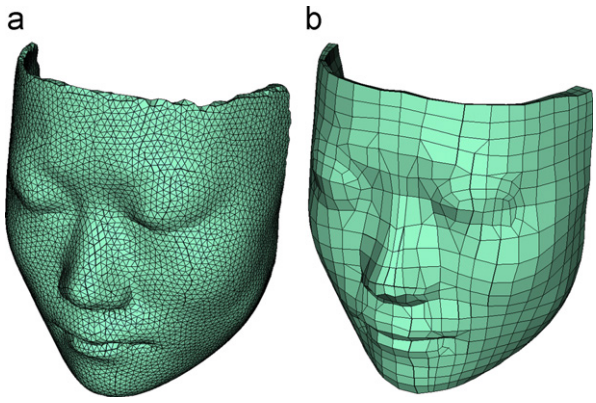

Fig. 11. Third individual facial model (a) and its hexahedral meshing result with our approach (b).

initial tetrahedral mesh for the second (resp. third) individual facial model and its hexahedral dominant meshing results. We can observe that, although the individual models are different from the generic model, our approach works well and generates appropriate mesh structures for important anatomical features such as the eyes, nose and mouth.

5. Conclusions

This paper presents a novel method to generate patient-specific hexahedral meshes of facial soft tissue models, based on a volumetric cross-parameterization mapping from a standard hexahedral mesh to the individual model. The volumetric parameterization is composed of triple of the volumetric harmonic fields, the conjugation of which is improved by solving the Poisson equations to achieve some quasi-conformal mapping effect. In addition, some piecewise constraints on the harmonic fields are added to ensure anatomical feature correspondence. The experiments demonstrate that our method can generate high quality hexahedral meshes for patient-specific facial models, avoid element flipping and preserve mesh element angles to a significant extent. Finally, we can assign the hexahedral meshes generated with anisotropic materials and make biomechanical analysis simulations for individual facial soft tissues.

Future works involve extending the proposed method to models of other shapes, where the volumetric domain may be very different from a unit cube domain. Note that the parameterization domain needs not to be a unit cube domain, but can be a domain such as a cylinder domain for a long bone, which should fit the model morphology. In the future, we will focus on more precise anatomical feature alignment mechanisms, which may rely on material information. Furthermore, the system's interface will be improved to generate the hexahedral mesh for specific models more easily.

Acknowledgements

This research was supported by the National Natural Science Foundation (nos. 60873126 and 60903136), the Doctorial subject special scientific research fund of Education Ministry (no. 20070335074) and the Postdoctoral Science Foundation (no. 20080441236) of China.

References

[1] Alliez P, Cohen-Steiner D, Yvinec M, Desbrun M. Variational tetrahedral meshing. ACM Trans Graph 2005;24(3):617–25.
[2] Du Q, Wang D. Tetrahedral mesh generation and optimization based on centroidal Voronoi tessellations. Int J Numer Methods Eng 2003;56(9): 1355–73.
[3] Shewchuk JR. Tetrahedral mesh generation by Delaunay refinement. In: Proceedings of the 14th annual ACM symposium on computational geometry, Minneapolis, Minnesota, USA; 1998. p. 86–95.
[4] Lu Y, Gadh R, Tautges TJ. Feature based hex meshing methodology: feature recognition and volume decomposition. Comput Aided Des 2001;33(3): 221–32.
[5] Price MA, Armstrong CG. Hexahedral mesh generation by medial surface subdivision: Part I. Int J Numer Methods Eng 1995;38:3335–59.
[6] Price MA, Armstrong CG. Hexahedral mesh generation by medial surface subdivision: Part II. Int J Numer Methods Eng 1997;40:111–36.
[7] Blacker TD, Meyers RJ. Seams and wedges in plastering: a 3-D hexahedral mesh generation algorithm. Eng. Comput. 1993;9:83–93.
[8] Schneiders R. A grid-based algorithm for the generation of hexahedral element meshes. Eng Comput 1996;12:168–77.
[9] Tautges TJ, Blacker T, Mitchell S. The whisker-weaving algorithm: a connectivity based method for constructing all-hexahedral finite element meshes. Int J Numer Methods Eng 1996;39:3327–49.
[10] Shepherd JF, Johnson CR. Hexahedral mesh generation constraints. Eng Comput 2008;24(3):195–213.
[11] Couteau B, Payan Y, Lavalle S. The mesh-matching algorithm: an automatic 3d mesh generator for finite element structures. J Biomech 2000;33:1005–9.
[12] Chabanas M, Luboz V, Payan Y. Patient specific finite element model of the face soft tissues for computer-assisted maxillofacial surgery. Med Image Anal 2003;7:131–51.
[13] Yang Y-L, Kim J, Luo F, Hu S-M, Gu X. Optimal surface parameterization using inverse curvature map. IEEE Trans Visualiz Comput Graph 2008;14(5): 1054–66.
[14] Ray N, Li W-C, Lévy B, Sheffer A, Alliez P. Periodic global parameterization. ACM Trans Graph 2006;25(4):1460–85.
[15] Kälberer F, Nieser M, Polthier K. QuadCover—surface parameterization using branched coverings. Comput Graph Forum 2007;26(3):75–384.
[16] Gu X, Yau S-T. Global conformal surface parameterization. In: Proceedings of eurographics symposium on geometry processing, Aachen, Germany; 2003. p. 127–37.
[17] Lai Y-K, Hu S-M, Pottmann H. Surface fitting based on a feature sensitive parameterization. Comput Aided Des 2006;38(7):800–7.
[18] Li X, Guo X, Wang H, He Y, Gu X, Qin H. Harmonic volumetric mapping for solid modeling applications. In: Proceedings of the 2007 ACM symposium on solid and physical modeling, Beijing, China; 2007. p. 109–20.
[19] He Y, Yin X, Luo F, Gu X. Harmonic Volumetric parameterization using Green's functions on star shapes. In: Symposium on geometry processing, Copenhagen, Denmark; 2008.
[20] Kraevoy V, Sheffer A. Cross-parameterization and compatible remeshing of 3D models. ACM Trans Graph. 2004;23(3):861–9.
[21] Martin T, Cohen E, Kirby M. Volumetric parameterization and trivariate B-spline fitting using harmonic functions. In: Proceedings of the 2008 ACM symposium on solid and physical modeling, New York, NY, USA; 2008. pp. 269–80.
[22] Lévy B, Liu Y. Lp Centroidal Voronoi Tesselation and its applications. ACM Trans Graph (Proceedings ACM SIGGRAPH) 2010.
[23] Huang J, Shi X, Liu X, Zhou K, Wei L-Y, Teng S, et al. Subspace gradient domain mesh deformation. ACM Trans Graph (Proceedings ACM SIGGRAPH) 2006;25(3):1126–34.
[24] Huang J, Liu X, Jiang H, Wang Q, Bao H. Gradient-based shell generation and deformation. Comput Animat Virtual Worlds 2007;18(4–5):301–9.
[25] Han S, Xia J, He Y. Hexahedral shell mesh construction via volumetric polycube map. In: Proceedings of the 2007 ACM symposium on solid and physical modeling, Haifa, Israel; 2010. p. 109–20.
[26] Zhang M, Huang J, Liu X, Bao H. A wave-based anisotropic quadrangulation method. ACM Trans Graph (Proceedings ACM SIGGRAPH) 2010.
[27] Bommes D, Zimmer H, Kobbelt L. Mixed-integer quadrangulation. ACM Trans Graph (Proceedings ACM SIGGRAPH) 2009.
[28] Knupp PM. Algebraic mesh quality metrics for unstructured initial meshes. Finite Elem Anal Des 2003;39:217–41.
[29] Meyer M, Desbrun M, Schroder P, Barr AH. Discrete differential-geometry operators for triangulated 2-manifolds. In: Hege H-C, Polthier K, editors. Visualization and mathematics III. Heidelberg: Springer; 2003. p. 35–57.
[30] Wang Y, Gu X, Yau S-T. Volumetric harmonic map. Commun Inf Syst 2004;3(3): 191–202.
[31] Liao S-H, Tong R-F, Dong J-X. Gradient field based inhomogeneous volumetric mesh deformation for maxillofacial surgery simulation. Comput Graph 2009;33:424–32.